Using pano-mapping tables for unwarping of omni-images into panoramic and perspective-view images

S.W. Jeng and W.H. Tsai

Abstract: A unified approach to unwarping of omni-images into panoramic or perspective-view images is proposed. The approach does not adopt the conventional technique of calibrating the related parameters of an omni-camera. Instead, it is based on a new concept of a pano-mapping table, which is created once forever, by a simple learning process for an omni-camera of any kind, as a summary of the information conveyed by all the camera parameters. The learning process takes, as input, a set of landmark point pairs, in the world space and in a given image. With the help of the pano-mapping table, any panoramic or perspective-view image can be created from an input omni-image taken by the omni-camera, according to an analytic computation process proposed in the paper. Experimental results show the feasibility of the proposed approach.

1 Introduction

Omni-cameras are used in many applications, such as visual surveillance and robot vision [1–4], for taking omni-images of camera surroundings. Usually, there exists an extra need to create perspective-view images from omni-images for human comprehensibility or event recording. This work is called unwarping, which usually is a complicated work. Fig. 1 shows an example, where Fig. 1*a* is an omni-image and Fig. 1*b* a perspective-view image obtained from unwarping the image of Fig. 1*a* by a method proposed by the authors [9].

Omni-cameras can be categorised into two types according to the involved optics, namely, dioptric and catadioptric [6]. A dioptric omni-camera captures incoming light going directly into the imaging sensor to form omni-images. An example of dioptric omni-cameras is the fish-eye camera. A catadioptric omni-camera captures incoming light reflected by a mirror to form omni-images. The mirror surface may be in various shapes, like conic, hyperbolic etc. If all the reflected light rays pass through a common point, the camera is said additionally to be of the single-view point (SVP) type [5]; otherwise, of the non-single-view point (non-SVP) type.

The method for unwarping omni-images is different for each distinct type of omni-camera. Generally speaking, omni-images taken by the SVP catadioptric camera [6, 7] as well as the dioptric camera [11] are easier to unwarp than those taken by the non-SVP catadioptric camera [8, 9]. Conventional methods for unwarping omni-images require the knowledge of certain camera parameters, like the focal length of the lens, the coefficients of the mirror surface shape equation etc. to do calibration before the unwarping can be done [12–16]. However, in some situations, we cannot get all the information of the omni-camera parameters, and then the unwarping work cannot be conducted. It is desired to have a more convenient way to deal with this problem.

In this paper, we propose a unified approach to the unwarping of omni-images taken by all kinds of omni-cameras, by which it is unnecessary to know the camera parameters in advance. This is made possible by the use of a 'pano-mapping table' proposed in this study, which may be regarded as a summary of the information conveyed by all the camera parameters. The pano-mapping table is created 'once forever' for each omni-camera. And given an omni-image taken by the camera, the table may be utilised to unwarp the image in analytic ways, to create panoramic or perspective-view images from any viewpoints in the world space. The pano-mapping table is invariant in nature with respective to the camera position, i.e. it is not changed even when the camera is moved around. The table is created by a calibration process making use of certain selected points in the world space with known co-ordinates and their corresponding pixels in an omni-image.

2 Proposed method using pano-mapping table

The proposed method consists of three major stages: (i) landmark learning, (ii) table creation, and (iii) image unwarping.

(i) *Landmark learning:* This first step is a procedure in which some pairs of selected world space points with known positions and their corresponding pixels in a taken omni-image are set up. More specifically, the co-ordinates of at least five points, called 'landmark points' hereafter, which are easy to identify in the world space (for example, a corner in a room), are measured manually with respect to a selected origin in the world space, then the corresponding pixels of such landmark points in the taken

doi:10.1049/iet-ipr:20060201

Paper first received 25th June and in revised form 27th November 2006

The authors are with the Department of Computer Science, National Chiao Tung University, 1001 Ta Hsueh Road Hsinchu, Taiwan 30010, Republic of China

W. H. Tsai is also with the Department of Computer Science and Information Engineering Asia University Liufeng Road, Wufeng, Taichung, Taiwan 41354, Republic of China

E-mail: sunny@itri.org.tw

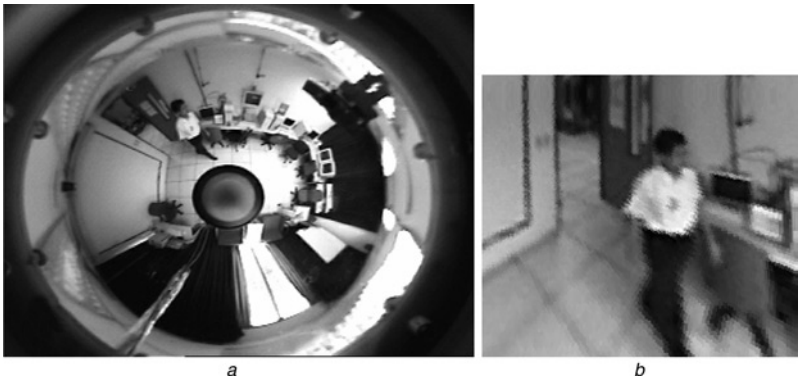

Fig. 1 *Example of image unwarping*

a Omni-image
b Perspective-view image resulting from unwarping a portion of the omni-image in *a*

omni-image are segmented out. A world space point and its corresponding image pixel so selected together are said to form a landmark point pair.

(ii) *Table creation:* This second step is a procedure in which a pano-mapping table is built using the co-ordinate data of the landmark point pairs. The table is 2-dimensional in nature with the horizontal and vertical axes specifying, respectively, the range of the azimuth angle θ as well as that of the elevation angle ρ of all possible incident light rays going through the mirror centre. An illustration is shown in Fig. 2, and an example of the pano-mapping table of size $M \times N$ is shown in Table 1. Each entry E_{ij}, with indices (i, j) in the pano-mapping table, specifies an azimuth-elevation angle pair $(\boldsymbol{\theta}_i, \boldsymbol{\rho}_j)$, which represents an infinite set S_{ij} of world space points passing through by the light ray with azimuth angle $\boldsymbol{\theta}_i$ and elevation angle $\boldsymbol{\rho}_j$ These world space points in S_{ij} are all projected onto an identical pixel P_{ij} in any omni-image taken by the camera, forming a pano-mapping f_{pm} from S_{ij} to P_{ij}. An illustration is shown in Fig. 3. This mapping is shown in the Table by filling entry E_{ij} with the co-ordinates (u_{ij}, v_{ij}) of pixel P_{ij} in the omni-image. The Table as a whole specifies the nature of the omni-camera, and may be used to create any panoramic or perspective-view images, as described subsequently.

(iii) *Image unwarping:* This third step is a procedure in which the pano-mapping table T_{pm} of an omni-camera is used as a medium to construct a panoramic or perspective-view image Q of any size for any viewpoint from a given omni-image I taken by the omni-camera. The basic concept in the procedure is to *map* each pixel q in Q to an entry E_{ij} with co-ordinate values (u_{ij}, v_{ij}) in the pano-mapping table T_{pm} and to assign the colour value of the pixel at co-ordinates (u_{ij}, v_{ij}) of image I to pixel q in Q. Details of each stage are given in the following.

Table 1: Example of pano-mapping table of size $M \times N$

	θ_1	θ_2	θ_3	θ_4	...	θ_M
ρ_1	(u_{11}, v_{11})	(u_{21}, v_{21})	(u_{31}, v_{31})	(u_{41}, v_{41})	...	(u_{M1}, v_{M1})
ρ_2	(u_{12}, v_{12})	(u_{22}, v_{22})	(u_{32}, v_{32})	(u_{42}, v_{42})	...	(u_{M2}, v_{M2})
ρ_3	(u_{13}, v_{13})	(u_{23}, v_{23})	(u_{33}, v_{33})	(u_{43}, v_{43})	...	(u_{M1}, v_{M3})
ρ_4	(u_{14}, v_{14})	(u_{24}, v_{24})	(u_{34}, v_{34})	(u_{44}, v_{44})	...	(u_{M1}, v_{M4})
...	...	...	...	...	...	...
ρ_N	(u_{1N}, v_{1N})	(u_{2N}, v_{2N})	(u_{3N}, v_{3N})	(u_{4N}, v_{4N})	...	(u_{MN}, v_{MN})

2.1 Landmark learning procedure

Before describing the landmark learning procedure, we briefly explain the system configuration as shown in Fig. 2. A 'downward-looking' omni-camera is attached 'horizontally' at the ceiling centre of a room, with both its mirror-base plane and omni-image plane parallel to the floor, which is just the X-Y plane of the world co-ordinate system with its co-ordinates denoted by (X, Y, Z) and its origin by O_w. The mirror centre of the omni-camera, denoted as O_m, is located at $(-D, 0, H)$ with respect to O_w in the world co-ordinate system. A camera co-ordinate system is set up at O_m, with its co-ordinates denoted by (x, y, z) and its three axes all parallel to those of the

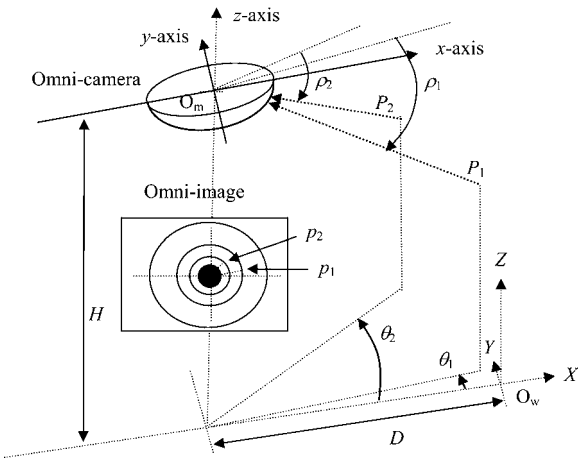

Fig. 2 *System configuration*

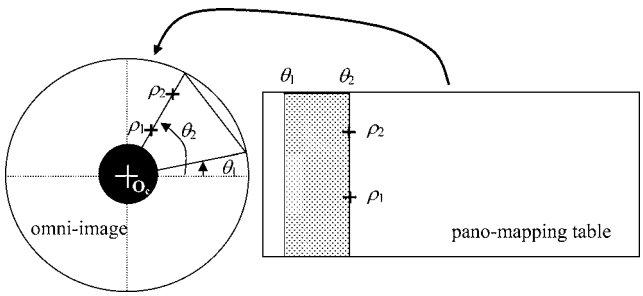

Fig. 3 *Mapping between pano-mapping table and omni-image*

world co-ordinate system. Also shown in the Figure as an illustration of the definitions of the azimuth and elevation angles are two points P_1 and P_2 in the world space, with corresponding image points P_1 and P_2 in the omni-image. The elevation angles of P_1 and P_2 with respect to the horizontal base plane of the mirror are $\boldsymbol{\rho}_1$ and $\boldsymbol{\rho}_2$, respectively, and their azimuth angles with respect to the x-axis of the camera co-ordinate system are θ_1 and θ_2, respectively.

The landmark learning procedure proceeds, at first, by selecting a sufficient number (≥ 5) of landmark point pairs, with the world space points being easy to identify. The co-ordinates of the world space points are then measured. Fig. 4 shows the interface we have designed for acquiring the data of the landmark point pairs easily. Especially, note that, in Fig. 3, the mirror centre O_m of the camera with known world co-ordinates (X_0, Y_0, Z_0) just appears to be the image centre O_c with known co-ordinates (u_0, v_0). This image centre can be automatically extracted by a simple image analysis scheme [18, 19]. We skip the detail here and take the co-ordinate data of the point pair (O_c, O_m) as the first set of the learned data. After learning, assume that we have n sets of landmark point pair data, each set including the co-ordinates (u_k, v_k) and (X_k, Y_k, Z_k) of the image point and the corresponding world space point, respectively, where $k = 0, 1, \ldots, n-1$.

2.2 Table creation procedure

The pano-mapping table is a two-dimensional array, for use as a medium for unwarping omni-images after it has been constructed. We may imagine the table as a longitude and latitude system with a horizontal θ-axis and a vertical ρ-axis, specifying the azimuth and elevation angles of incident light rays through the mirror centre, as mentioned previously. We divide the range 2π rad (360°) of the azimuth angles equally into M units, and the range of the elevation angles, say from $\boldsymbol{\rho}_s$ to $\boldsymbol{\rho}_e$, into N units, to create a table T_{pm} of $M \times N$ entries. Each entry E with corresponding angle pair (θ, ρ) in T_{pm} maps to a pixel p with co-ordinates (u, v) in the input omni-image I. This mapping f_{pm} may be decomposed into two separate mappings, one in the azimuth direction and the other in the radial direction, called azimuth-directional mapping and radial-directional mapping, respectively.

Owing to the rotation-invariant property of the omni-camera, the azimuth angle θ of each world space point through which the light ray passes is actually identical to the angle ϕ of the corresponding pixel p with respect to the u-axis in the input image I, i.e. the azimuth-directional mapping is just an identity function f_a, such that $f_a(\theta) = \phi = \theta$.

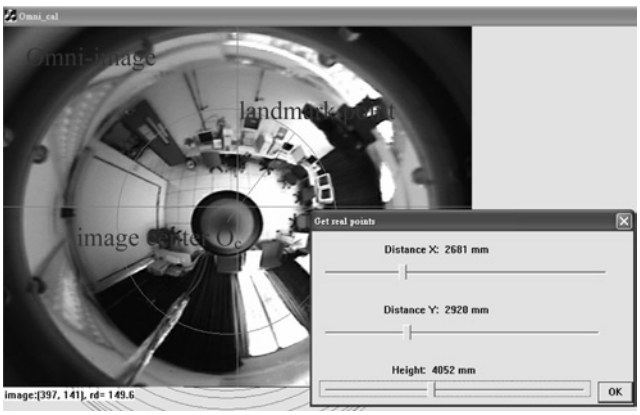

Fig. 4 *Landmark learning interface*

On the other hand, because of the nonlinear property of the mirror surface shape, the radial-directional mapping should be specified by a nonlinear function f_r, such that the radial distance r from each image pixel p with co-ordinates (u, v) in I to the image centre O_c at (u_0, v_0) may be computed by $r = f_r(\boldsymbol{\rho})$. Based on the two mappings f_a and f_r, we can regard the pairs $(r, \phi) = (f_r(\boldsymbol{\rho}), \theta)$ of all the image pixels to form a polar co-ordinate system with the image co-ordinates (u, v) specified by

$$\begin{aligned} u &= r \times \cos\phi = f_r(\boldsymbol{\rho}) \times \cos\theta, \\ v &= r \times \sin\phi = f_r(\boldsymbol{\rho}) \times \sin\theta \end{aligned} \tag{1}$$

In this study, we also call f_r a 'radial stretching function', and we attempt to describe it by the following 4th-degree polynomial function

$$r = f_r(\boldsymbol{\rho}) = a_0 + a_1 \times \rho^1 + a_2 \times \rho^2 + a_3 \times \rho^3 + a_4\rho^4 \tag{2}$$

where $a_0 - a_4$ are five coefficients to be estimated using the data of the landmark point pairs, as described in the following algorithm. A similar idea of approximation can be found in Scotti *et al.* [10]. Let the data of the n selected landmark point pairs be denoted as (P_0, p_0), (P_1, p_1), …, (P_{n-1}, p_{n-1}), where $n \geq 5$.

Algorithm 1. Estimation of coefficients of radial stretching function:

Step 1. *Co-ordinate transformation in world space*: Transform the world co-ordinates (X_k, Y_k, Z_k) of each selected landmark point P_k, $k = 1, 2, \ldots, n-1$, with respect to O_w into co-ordinates with respect to O_m by subtracting from (X_k, Y_k, Z_k) the co-ordinate values (X_0, Y_0, Z_0) = ($-D$, 0, H) of O_m. Hereafter, (X_k, Y_k, Z_k) will be used denote this co-ordinate transformation result.

Step 2. *Elevation angle and radial distance calculation:* Use the co-ordinate data of each landmark point pair (P_k, p_k), including the world co-ordinates (X_k, Y_k, Z_k) and the image co-ordinates (u_k, v_k), to calculate the elevation angle $\boldsymbol{\rho}_k$ of P_k in the world space and the radial distance r_k of p_k in the image plane by the following equations

$$\boldsymbol{\rho}_k = \tan^{-1}\left[\frac{Z_k}{D_k}\right] \tag{3}$$

$$r_k^2 = u_k^2 + v_k^2 \tag{4}$$

where D_k is the distance from the landmark point P_k to the mirror centre O_m in the X-Y plane of the world co-ordinate system, computed by $D_k = \sqrt{(X_k^2 + Y_k^2)}$.

Step 3. *Calculation of coefficients of the radial stretching function*: Substitute all the data ρ_0, ρ_2, …, ρ_{n-1} and r_1, r_2, …, r_{n-1} computed in the last step into (2) to get n simultaneous equations

$$\begin{aligned} r_0 &= f_r(\rho_0) = a_0 + a_1 \times \rho_0^1 + a_2 \times \rho_0^2 + a_3 \times \rho_0^3 + a_4\rho_0^4, \\ r_1 &= f_r(\rho_1) = a_0 + a_1 \times \rho_1^1 + a_2 \times \rho_1^2 + a_3 \times \rho_1^3 + a_4\rho_1^4, \\ &\vdots \\ r_{n-1} &= f_r(\rho_{n-1}) = a_0 + a_1 \times \rho_{n-1}^1 + a_2 \times \rho_{n-1}^2 \\ &\quad + a_3 \times \rho_{n-1}^3 + a_4\rho_{n-1}^4 \end{aligned}$$

and solve them to get the desired coefficients (a_0, a_1, a_2, a_3, a_4) of the radial stretching function f_r by a numerical analysis method [17].

Now, the entries of the pano-mapping table $T_{\rm pm}$ can be filled with the corresponding image co-ordinates using (1) and (2) by the following algorithm. Note that there are $M \times N$ entries in the table.

Algorithm 2. Filling entries of pano-mapping table:

Step 1. Divide the range 2π of the azimuth angles into M intervals, and compute the ith azimuth angle θ_i by

$$\theta_i = i \times (2\pi/M), \text{ for } i = 0,1,\ldots, M-1 \quad (5)$$

Step 2. Divide the range $[\boldsymbol{\rho}_e - \boldsymbol{\rho}_s]$ of the elevation angles into N intervals, and compute the jth elevation angle ρ_j by

$$\rho_j = j \times [(\boldsymbol{\rho}_e - \boldsymbol{\rho}_s)/N] + \boldsymbol{\rho}_s, \quad \text{for } j = 0, 1, \ldots, N-1 \quad (6)$$

Step 3. Fill the entry E_{ij} with the corresponding image co-ordinates (u_{ij}, v_{ij}) computed according to (1) and (2) as follows

$$u_{ij} = r_j \times \cos\ \theta_i,$$
$$v_{ij} = r_j \times \sin\ \theta_i \quad (7)$$

where r_j is computed by

$$r_j = f_{\rm r}(\rho_j) = a_0 + a_1 \times \rho_j^1 + a_2 \times \rho_j^2 + a_3 \times \rho_j^3 + a_4\rho_j^4 \quad (8)$$

with $(a_0,\ a_1,\ a_2,\ a_3,\ a_4)$ being those computed by Algorithm 1.

2.3 Image unwarping procedure

Now, we are ready to show how to reconstruct a panoramic or perspective-view image from an omni-image with the aid of a pano-mapping table. Three cases can be identified, as described in the following.

2.3.1 Generation of generic panoramic image from given omni-image: Given an input omni-image G and a pano-mapping table $T_{\rm pm}$, we may generate from G a corresponding generic panoramic image Q which is exactly of the same size $M\times\ N$ of $T_{\rm pm}$. The steps are as follows. First, for each entry E_{ij} of $T_{\rm pm}$ with azimuth angle θ_i and elevation angle ρ_j, take out the co-ordinates (u_{ij}, v_{ij}) filled in E_{ij}, then assign the colour values of the pixel p_{ij} of G at co-ordinates (u_{ij}, v_{ij}) to the pixel q_{ij} of Q at co-ordinates (i, j). After all entries of the table are processed, the final Q becomes a generic panoramic image corresponding to G. In this process, we may regard Q as the output of the pano-mapping $f_{\rm pm}$ described by the pano-mapping table $T_{\rm pm}$ with G as the input, i. e. $f_{\rm pm}(G) = Q$.

2.3.2 Generation of a specific panoramic image: With the aid of a pano-mapping table $T_{\rm pm}$ with $M \times N$ entries, we may also generate from a given omni-image G a panoramic image Q of any size, say $M_Q\times\ N_Q$, which is the panoramic projection of the original scene appearing in G at any distance D with respect to the mirror centre O_m with a projection band of any height H. An illustration of such an imaging configuration from a lateral view is shown in Fig. 5.

The process for generating such an image is similar to that for generating the generic panoramic image described

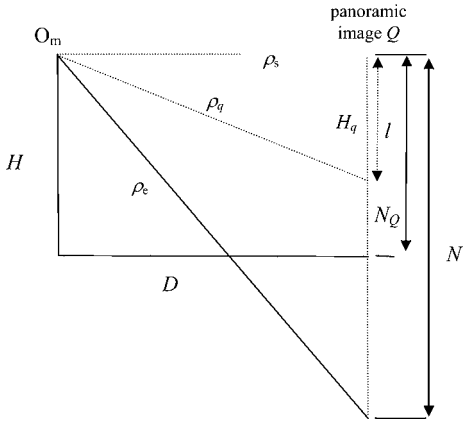

Fig. 5 *Lateral-view configuration for generating a panoramic image*

previously. First, we map each image pixel q_{kl} in Q at co-ordinates $(k,\ l)$ to an entry E_{ij} in $T_{\rm pm}$ filled with co-ordinates $(u_{ij},\ v_{ij})$, then we assign the colour value of the pixel p_{ij} of G at $(u_{ij},\ v_{ij})$ to q_{kl}. Mapping of q_{kl} to E_{ij} is based on the use of the knowledge of the parameters M_Q, N_Q, D and H, as well as some related principles like triangulation, proportionality etc.

In more detail, as the azimuth angle range 2π is divided into M_Q intervals in image Q, the image pixel q_{kl} at co-ordinates $(k,\ l)$ is, by linear proportionality, the projection result of a light ray R_q with an azimuth angle $\theta_q K \times (2\pi/M_{\rm Q})$. As each azimuth angle interval in $T_{\rm pm}$ is $2\pi/M$, the index I of the corresponding entry E_{ij} in $T_{\rm pm}$ with the azimuth angle of $\theta_{\rm q}$ is

$$i = \theta_q/(2\pi/M) = [k \times (2\pi/M_Q)]/(2\pi/M) = k \times \frac{M}{M_Q} \quad (9)$$

where we assume M is a multiple of M_Q. If this is not the case, the right-hand side of (9) should be replaced with its integer floor value.

Next, we have to compute the elevation angle $\boldsymbol{\rho}_q$ of the aforementioned light ray R_q projecting onto pixel q_{kl}, to decide the index j of E_{ij}. For this, as the height of the projection band is H and image Q is divided into N_Q intervals, by linear proportionality again, we may compute the height of R_q at D as

$$H_q = l \times \frac{H}{N_Q} \quad (10)$$

then, by trigonometry, we have the elevation angle ρ_q as

$$\boldsymbol{\rho}_q = \tan^{-1}\left(\frac{H_q}{D}\right) \quad (11)$$

therefore we can compute the index j of E_{ij} by proportionality again as

$$j = (\boldsymbol{\rho}_q - \boldsymbol{\rho}_s)/[\boldsymbol{\rho}_e - \boldsymbol{\rho}_s)/N] = \frac{(\boldsymbol{\rho}_q - \boldsymbol{\rho}_s) \times N}{(\boldsymbol{\rho}_e - \boldsymbol{\rho}_s)} \quad (12)$$

because the elevation angle range $\boldsymbol{\rho}_{\rm e} - \boldsymbol{\rho}_{\rm s}$ is divided into N intervals. In case the right side of (12) is not an integer, it should be replaced by its integer floor value.

With the indices (i, j) of E_{ij} available, the content of E_{ij}, i. e. the co-ordinates (u_{ij}, v_{ij}), may be obtained. And, finally, the colour value of the omni-image G at (u_{ij}, v_{ij}) is assigned to the pixel q_{kl} at co-ordinates (k, l) of Q. After all pixels of Q are processed in this way, the final content of Q is just the desired panoramic image.

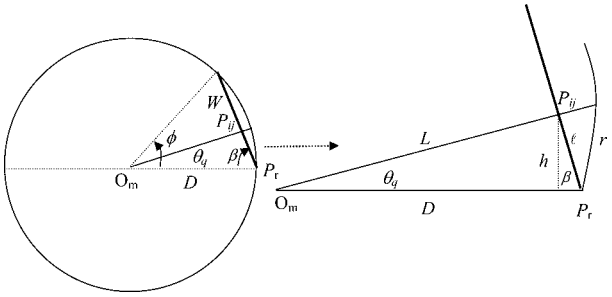

Fig. 6 *Top-view configuration for generating perspective-view image*

2.3.3 Generation of specific perspective-view image: Given an omni-image G and a pano-mapping table T_{pm} with $M \times N$ entries, we may also generate from G a perspective-view image Q of any size $M_Q \times N_Q$, which is the perspective projection of the original scene appearing in G onto a planar rectangular region A_{P} of any size $W \times H$ at any distance D with respect to the mirror centre O_m. A top-view of the configuration for such an image generation process is shown in Fig. 6. The idea again is to map each image pixel q_{kl} in Q at co-ordinates (k, l) to an entry E_{ij} in T_{pm} filled with co-ordinates (u_{ij}, v_{ij}), and then to assign the colour value of the pixel p_{ij} of G at (u_{ij}, v_{ij}) to q_{kl}. Mapping of q_{kl} to E_{ij} is accomplished via the steps of computing the azimuth and the elevation angles θ_q and ρ_q associated with E_{ij} and corresponding to q_{kl}.

Referring to Fig. 6, we first calculate the angle ϕ in the Figure. By trigonometry, we have

$$W^2 = D^2 + D^2 - 2 \times D \times D \times \cos\phi$$

from which, ϕ may be solved to be

$$\phi = \cos^{-1}\left[1 - \frac{W^2}{2 \times D^2}\right] \tag{13}$$

Also, it is easy to see from the Figure that

$$\beta = \frac{\pi - \phi}{2} \tag{14}$$

Next, we compute the index i of entry E_{ij} of table T_{pm} corresponding to pixel q_{kl} in image Q. First, let P_{ij} denote the intersection point of the light ray R_q projecting onto q_{kl} and the planar projection region A_{p}. Note that each entry E_{ij} has a corresponding P_{ij}, then we compute the distance ℓ between point P_{ij} and the border point P_r shown in Fig. 6 by linear proportionality as

$$\ell = k \times \frac{W}{M_Q} \tag{15}$$

as the projection region A_{p} has a width of W, the image Q has a width of M_Q pixels, and pixel q_{kl} has an index of k in the horizontal direction.

Also, by trigonometry we can compute the distance L between point P_{ij} and the mirror centre O_m as

$$L = \sqrt{D^2 + \ell^2 - 2 \times \ell \times D \times \cos\beta} \tag{16}$$

and then the distance h from point P_{ij} to the line segment $\overline{O_m P_r}$ connecting O_m and P_r as

$$h = \ell \times \sin\beta \tag{17}$$

Hence, the azimuth angle θ_q of point P_{ij} with respect to $\overline{O_m P_r}$ satisfies

$$\sin\theta_q = \frac{h}{L} = \frac{\ell \times \sin\beta}{\sqrt{D^2 + \ell^2 - 2 \times \ell \times D \times \cos\beta}}$$

which leads to

$$\theta_q = \sin^{-1}\left[\frac{\ell \times \sin\beta}{\sqrt{D^2 + \ell^2 - 2 \times \ell \times D \times \cos\beta}}\right] \tag{18}$$

Finally, the index i of entry E_{ij} may computed by linear proportionality as

$$i = \left[\frac{\theta_q}{2\pi}\right] \times M \tag{19}$$

where we assume the right-hand side of the equality is an integer. If this is not the case, it should be replaced by its integer floor value.

As to the index j of E_{ij}, it can be computed in a way similar to that for deriving (10), (11) and (12) as follows

$$H_q = l \times \frac{H}{N_Q} \tag{20}$$

$$\boldsymbol{\rho}_q = \tan^{-1}\left[\frac{H_q}{L}\right] \tag{21}$$

$$j = \frac{(\boldsymbol{\rho}_q - \boldsymbol{\rho}_s) \times N}{(\boldsymbol{\rho}_e - \boldsymbol{\rho}_s)} \tag{22}$$

With the indices (i, j) of E_{ij} ready, finally we can obtain the co-ordinates (u_{ij}, v_{ij}) in E_{ij} and assign the colour value of the image pixel p_{ij} of G at co-ordinates (u_{ij}, v_{ij}) to pixel q_{kl} of Q at co-ordinates (k, l). After all pixels of Q are processed, the final content of Q is just the desired perspective-view image.

3 Experimental results

In our experiments, before performing the unwarping procedure, we carry out the landmark learning and the table creation procedures first. For these works, we provide a user-friendly interface as shown in Fig. 4, which can be used for identifying appropriate landmark pairs, as described in Section 2.1. Fig. 7*a* shows the final result of the learning procedure. Ten landmark point pairs were identified, as shown in the Figure. Also, the co-ordinates of the image centre, as well as the length of the 'cut-off radius' within which the omni-image is invisible because of the self-occlusion of the omni-camera, are extracted automatically in the learning procedure using an algorithm developed in this study [18, 19]. The region within the cut-off radius is marked by a circle with the co-ordinate values of the image centre and the radius length printed at the bottom of Fig. 7*a*. We used the cut-off radius to calculate one end $\boldsymbol{\rho}_e$ of the full range of the elevation angles. The learned landmark point pairs were used to estimate the coefficients of the radial stretching function as described by (2) in Section 2.2. Fig. 7*b* shows the fitted curve with the 10 learned landmark points superimposed on the drawing (marked with '+').

With the coefficients estimated, (1) and (2) were used to construct a pano-mapping table, as described in Section 2.2. The pano-mapping table can be used to unwarp an input omni-image into a panoramic or perspective-view image of any viewpoint, as described in Section 2.3. Fig. 8 shows some examples of images obtained from unwarping the omni-image shown in Fig. 8*c*. Fig. 8*a* is a generated

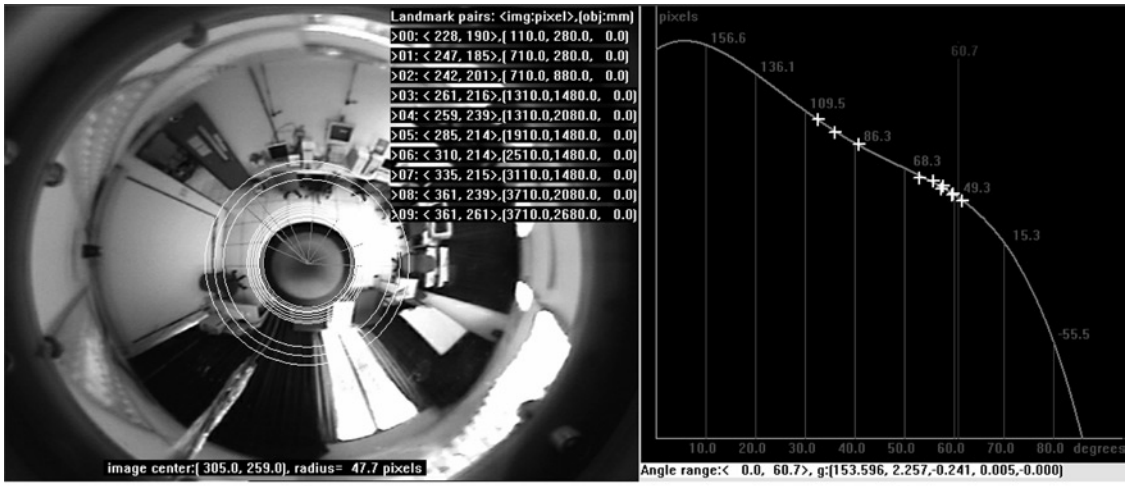

Fig. 7 *Landmark calibration*

a Landmark pairs
b Fitted radial stretching function

generic panoramic image. Note that this image is unique for an omni-camera. Fig. 8*b* is a panoramic image viewed at distance 184.1 cm with respect to the mirror centre O_m of the omni-camera with a projection height of 208.5 cm. Fig. 8*d* is a perspective-view image viewed at distance 184.1 cm with respect to the camera in a projection region of 216.3 × 208.5 cm^2. Note that Figs. 8*b* and 8*d* will look different by changing the relative positions with respect to the omni-camera. For example, Fig. 10 shows some perspective-view images generated from an omni-image video sequence at different projection distances.

The results shown in Fig. 8 can be compared with those of one conventional calibration method proposed by Mashita *et al*. [14], as shown in Fig. 9. There is difficulty to tell which of the reconstructed images in Figs. 8*d* and 9*d* is better, but we can be sure that the proposed method is a relatively simple and generic solution for all kinds of omni-cameras and no *a priori* knowledge about the used omni-camera is needed in the proposed method. This is really a great merit of the proposed method, which is not found in other methods.

4 Conclusions and discussions

A new approach to unwarping of omni-images taken by all kinds of omni-cameras is proposed. The approach is based on the use of pano-mapping tables proposed in this study, which may be regarded as a summary of the information

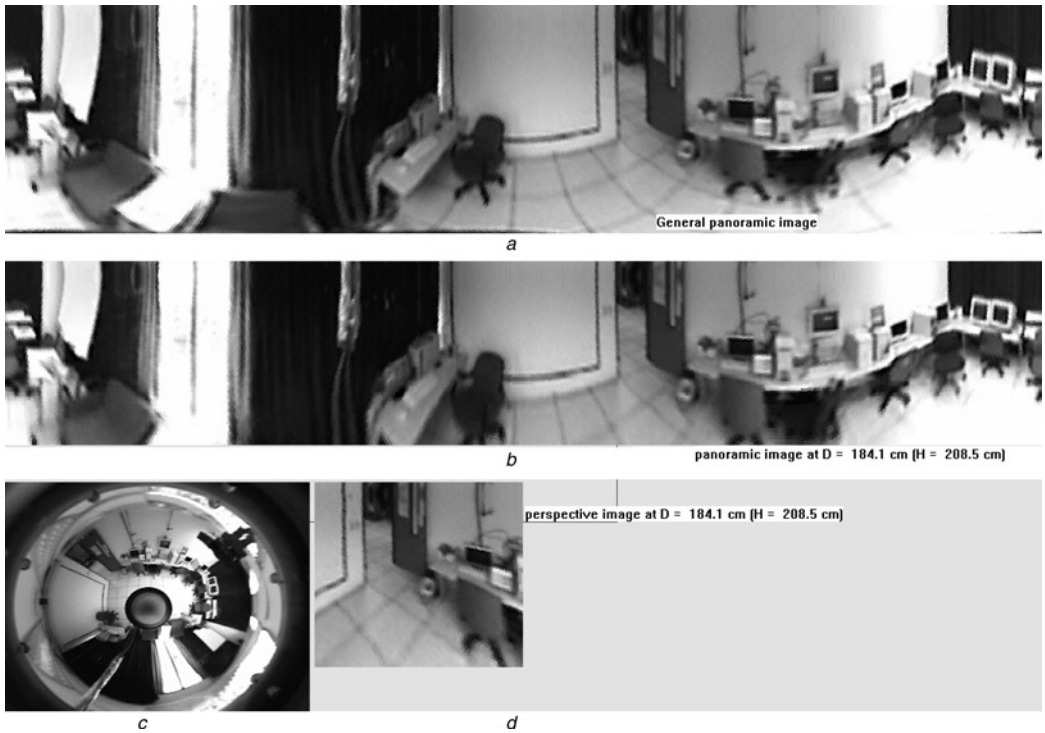

Fig. 8 *Examples of image unwarping*

a Generated generic panoramic image
b Generated panoramic image at distance 184.1 cm
c Original omni-image
d Generated perspective-view image

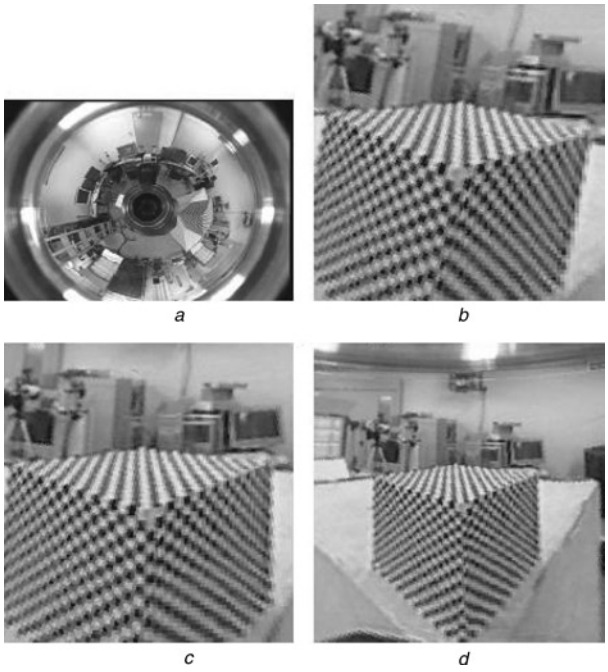

Fig. 9 *Unwarped perspective images using Mashita's calibration method*

a Orignal omni-image
b Unwarping result by treating the camera as an SVP omni-camera
c Best result by manually adjusting some parameters in the case of *b*
d Unwarping result using calibrated parameters

Fig. 10 *Perspective-view images generated from an omni-image video sequence taken by a tracking system*

These images can be considered as some snapshots of a video

conveyed by all the parameters of an omni-camera. The pano-mapping table is created once forever, for each omni-camera, and can be used to construct panoramic or perspective-view images of any viewpoint in the world space. This is a simple and efficient way to unwarping an omni-image taken by any omni-camera, when some of the physical parameters of the omni-camera cannot be obtained.

A possible application of this approach is panoramic imaging in a visual surveillance system in a room [20]. We tried this idea in this study, and the experimental results shown previously come from this test. Fig. 10 shows some perspective-view snapshots generated from the taken videos of the surveillance system, which are useful for identifying specific persons or for activity monitoring. As the snapshots are unwarping results from a portion of an omni-image, their image qualities are not so good, compared with images taken by a normal camera. If this issue is to be solved, we may add a pan-tilt-zoom camera into the surveillance system [10] to capture images of higher quality corresponding to the tracked versions of the perspective-view snapshots.

5 References

1 Benosman, R., and Kang, S.B.: 'Panoramic vision: Sensor, theory and applications'. Monographs in Computer Science (Springer-Verlag, New York, 2001)
2 Morita, S., Yamazawa, K., and Yokoya, N.: 'Networked video surveillance using multiple omnidirectional cameras'. Proc., IEEE Int. Symp. Comput. Intell. Robot. Autom., Kobe, 16–20 July 2003, Japan, pp. 1245–1250
3 Tang, L., and Yuta, S.: 'Indoor navigation for mobile robots using memorized omni-directional images and robot's motion'. Proc. IEEE/RSJ Int. Conf. Intell. Robots Syst., 30 September–5 October 2002, vol. 1, pp. 269–274
4 Winter, N., Gaspar, J., Lacey, G., and Santos-Victor, J.: 'Omnidirectional vision for robot navigation'. Proc. IEEE Workshop Omnidirectional Vision, OMNIVIS, South Carolina, USA, June 2000, pp. 21–28
5 Baker, S., and Nayar, S.K.: 'A theory of single-viewpoint catadioptric image formation', *Int. J. Comput. Vis.*, 1999, **35**, (2), pp. 175–196
6 Nayar, S.K.: 'Catadioptric omni-directional camera'. Proc. IEEE Conf. Comput. Vis. Pattern Recognit., San Juan, Puerto Rico, June 1997, pp. 482–488
7 Onoe, Y., Yokoya, N., Yamazawa, K., and Takemura, H.: 'Visual surveillance and monitoring system using an omni-directional video camera'. Proc. 14th Int. Conf. Pattern Recognit., Brisbane, Australia 16-20 August, vol. 1, pp. 588–592
8 Jeng, S.W., and Tsai, W.H.: 'Precise image unwarping of omni-directional cameras with hyperbolic-shaped mirrors'. Proc. 16th IPPR Conf. Comput. Vis., Graphics Image Process., Kinmen, Taiwan, 17–19 August 2003, pp. 414–422
9 Jeng, S.W., and Tsai, W.H.: 'Construction of perspective and panoramic images from omni-images taken from hypercatadioptric cameras for visual surveillance'. Proc. 2004 IEEE Int. Conf. on Netw. Sensing, Control, Taipei, Taiwan, 21–23 March 2004, pp. 204–209
10 Scotti, G., Marcenaro, L., Coelho, C., Selvaggi, F., and Regazzoni, C.S.: 'Dual camera intelligent sensor for high definition 360 degrees surveillance', *IEE Proc., Vis. Image Signal Process.*, 2005, **152**, (2), pp. 250–257
11 Mundhenk, T.N., Rivett, M.J., Liao, X., and Hall, E.L.: 'Techniques for fisheye lens calibration using a minimal number of measurements'. Proc. SPIE Intell. Robot. Comput. Vis. Conf. XIX, 2000, Boston, MA
12 Ying, X.H., and Hu, Z.Y.: 'Catadioptric camera calibration using geometric invariants', *IEEE Trans. Pattern Anal. Mach. Intell.*, 2004, **26**, (10), pp. 1260–1271
13 Geyer, C., and Daniilidis, K.: 'Catadioptric camera calibration'. Proc. IEEE 7th Int. Conf. Comput. Vis., September 1999, pp. 398–404
14 Mashita, T., Iwai, Y., and Yachida, M.: 'Calibration method for misaligned catadioptric camera', *IEICE Trans. Inf. Syst.*, 2006, **E89-D**, (7), pp. 1984–1993
15 Strelow, D., Mishler, J., Koes, D., and Singh, S.: 'Precise omnidirectional camera calibration,'. Proc. IEEE Conf. Comput. Vis. Pattern Recognit. (CVPR 2001), Kauai, HI, December 2001, vol. 1, pp. 689–694
16 Scaramuzza, D., Martinelli, A., and Siegwart, R.: 'A flexible technique for accurate omnidirectional camera calibration and structure from motion'. Proc. Fourth IEEE Int. Conf. Comput. Vis. Syst., 2006
17 Burden, L.R., and Faires, J.D.: 'Numerical analysis' (Brooks Cole, Belmont, CA, 2000. 7th edn.), ISBN: 0534382169
18 Zelniker, E., and Clarkson, I.: 'Maximum-likelihood estimation of circle parameters via convolution', *IEEE Trans. Image Process.*, 2006, **4**, (15), pp. 865–876
19 Kerbyson, D.J., and Atherton, T.J.: 'Circle detection using Hough transform filters'. Fifth Int. Conf. Image Process. Appl., Edinburgh, UK, 4–6 July 1995, pp. 370–374
20 Chen, X., and Tang, J.: 'Towards monitoring human activities using an omnidirectional camera'. Int. Conf. Multimodal Interfaces, Pittsburgh, 2002, pp. 423–428